

Radiation-induced magnetoresistance oscillation in a two-dimensional electron gas in Faraday geometry

X.L. Lei and S.Y. Liu

Department of Physics, Shanghai Jiaotong University, 1954 Huashan Rd., Shanghai 200030, China

Microwave-radiation induced giant magnetoresistance oscillations recently discovered in high-mobility two-dimensional electron systems in a magnetic field, are analyzed theoretically. Multiphoton-assisted impurity scatterings are shown to be the primary origin of the oscillation. Based on a model which considers the interaction of electrons with the electromagnetic fields in Faraday geometry, we are able not only to reproduce the correct period, phase and the negative resistivity of the main oscillation, but also to obtain secondary peaks and additional maxima and minima in the resistivity curve, some of which were already observed in the experiments.

PACS numbers: 73.50.Jt, 73.40.-c, 78.67.-n, 78.20.Ls

The discovery of a new type of magnetoresistance oscillations in a high mobility two-dimensional (2D) electron gas (EG) subjected to crossed microwave (MW) radiation field and a magnetic field,¹ especially the recent observation of peculiar "zero-resistance" states developed from the oscillation minima,^{2,3} has stimulated tremendous interest in the physics community.^{4,5,6,7,8,9} These magnetoresistivity oscillations were found to be accurately periodical in inverse magnetic field $1/B$. However, unlike the well-known Shubnikov-de Haas (SdH) oscillations whose period is determined by the electron density N_e ,¹⁰ the period of the radiation-induced oscillations is determined by the MW frequency ω . Also different from the possible cyclotron resonances of the high frequency (HF) field and its harmonics, which, if any, should appear as sharp peaks in the photoresistance at positions $\omega = j\omega_c$ (ω_c is the cyclotron frequency, $j = 1, 2, 3, \dots$),¹¹ the radiation-induced oscillations exhibit a smooth magnetic-field variation with the resistivity maxima at $\omega/\omega_c = j - \delta_1$ and minima at $\omega/\omega_c = j + \delta_2$ having positive δ_1 and δ_2 around $\frac{1}{4}$.² The resistivity minimum goes downward with increasing mobility and/or increasing radiation intensity until a "zero-resistance" state shows up, while the Hall resistivity keeps the classical form $R_{xy} = B/eN_e$ with no sign of quantum Hall plateau over the whole magnetic field range exhibiting resistivity oscillation.

To understand the origin of these unexpected oscillations and the "zero-resistance" states, different mechanisms have been suggested from intuitive models to microscopic calculations.^{4,5,6,7,8,9} Ref.4,5,6,7 proposed that the periodical structure of the density of states (DOS) of the 2DEG in a magnetic field and the photon-excited disorder-scattered electrons are the origin of the magnetoresistance oscillations. Durst *et. al.*⁴ presented a microscopic analysis for the conductivity assuming a δ -correlated disorder and a simple form of the 2D electron self-energy oscillatory with magnetic field, obtaining the correct period and phase, as well as the negative resistance at the locations of the experimentally observed "zero-resistance" states. Shi and Xie⁷ reported a similar result using the Tien and Gorden current formula¹²

for photon-assisted coherent tunneling. In these studies, however, the magnetic field is to provide a oscillatory DOS only and the HF field enters as if there is without magnetic field or with a magnetic field in Voigt configuration. The experimental setup requires to deal with the magnetic field \mathbf{B} which is perpendicular to the HF field $\mathbf{E}_s \sin \omega t$. In this Faraday configuration, the moving electron with a velocity, e.g. $\mathbf{v}_1 \cos(\omega t)$, induced by the HF field in the 2DEG, experiences a Lorentz force, which gives rise to additional electron motion perpendicular to \mathbf{v}_1 and \mathbf{B} with a velocity $(\omega_c/\omega)v_1 \sin(\omega t)$. In the range of $\omega \sim \omega_c$, the amplitudes of both velocities are of the same order of magnitude and are resonantly enhanced. Even if the cyclotron resonance (CR) may not show up in photoresistance in these high mobility systems at low temperatures, the CR of the HF current response is certainly there. Such an important effect will change the way how the HF photons assist the electron scattering in the Faraday configuration.

In this Letter, we propose a model for the interaction of electrons with the electromagnetic fields, demonstrating that in an electron gas having impurity and/or phonon scatterings, a HF field opens additional channels for electron transition between different states. Based on the theory developed for photon-assisted magnetotransport in Faraday geometry, which takes account of the CR of the HF current in 2DEG, we show that the main results of the experimentally observed radiation-induced magnetoresistivity oscillations can be well reproduced. We also obtain the secondary peaks and additional maxima and minima in the resistivity curve, some of which were already observed.

The experiments allow us to assume the 2DEG being in extended states over the magnetic field range relevant to this phenomenon. To give a general treatment, we consider N_e electrons in a unit area of a quasi-2D system in the x - y plane with a confining potential $V(z)$ in the z -direction. These electrons, besides interacting with each other, are scattered by random impurities/disorders and by phonons in the lattice. The experimental setup with MW illumination can be well modelled by applying a uniform dc electric field \mathbf{E}_0 and ac field $\mathbf{E}_t \equiv \mathbf{E}_s \sin(\omega t)$

of frequency ω in the x - y plane, together with a magnetic field $\mathbf{B} = (0, 0, B)$ along the z direction. In terms of the 2D center-of-mass momentum and coordinate of the electron system,^{13,14,16} which are defined as $\mathbf{P} \equiv \sum_j \mathbf{p}_{j\parallel}$ and $\mathbf{R} \equiv N_e^{-1} \sum_j \mathbf{r}_{j\parallel}$ with $\mathbf{p}_{j\parallel} \equiv (p_{jx}, p_{jy})$ and $\mathbf{r}_{j\parallel} \equiv (x_j, y_j)$ being the momentum and coordinate of the j th electron in the 2D plane, and the relative electron momentum and coordinate $\mathbf{p}'_{j\parallel} \equiv \mathbf{p}_{j\parallel} - \mathbf{P}/N_e$ and $\mathbf{r}'_{j\parallel} \equiv \mathbf{r}_{j\parallel} - \mathbf{R}$, the Hamiltonian of the system can be written as the sum of a center-of-mass part H_{cm} and a relative electron part H_{er} ($\mathbf{A}(\mathbf{r})$ is the vector potential of the \mathbf{B} field),

$$H_{\text{cm}} = \frac{1}{2N_e m} (\mathbf{P} - N_e e \mathbf{A}(\mathbf{R}))^2 - N_e e (\mathbf{E}_0 + \mathbf{E}_t) \cdot \mathbf{R}, \quad (1)$$

$$H_{\text{er}} = \sum_j \left[\frac{1}{2m} \left(\mathbf{p}'_{j\parallel} - e \mathbf{A}(\mathbf{r}'_{j\parallel}) \right)^2 + \frac{p_{jz}^2}{2m_z} + V(z_j) \right] + \sum_{i < j} V_c(\mathbf{r}'_{i\parallel} - \mathbf{r}'_{j\parallel}, z_i, z_j), \quad (2)$$

together with electron-impurity and electron-phonon interactions H_{ei} and H_{ep} . Here m and m_z are respectively the electron effective mass parallel and perpendicular to the plane, and V_c stands for the electron-electron Coulomb interaction. It should be noted that the uniform electric field (dc and ac) appears only in H_{cm} , and that H_{er} is just the Hamiltonian of a quasi-2D system subjected to a magnetic field. The coupling between the center-of-mass and the relative electrons exists via the electron-impurity and electron-phonon interactions. Our treatment starts with the Heisenberg operator equations for the rates of changes of the center-of-mass velocity $\dot{\mathbf{V}} = -i[\mathbf{V}, H] + \partial \mathbf{V} / \partial t$, with $\mathbf{V} = -i[\mathbf{R}, H]$, and of the relative electron energy $\dot{H}_{\text{er}} = -i[H_{\text{er}}, H]$, and proceeds with the determination of their statistical averages.

As proposed in Ref. 13, the center-of-mass coordinate \mathbf{R} and velocity \mathbf{V} can be treated classically, i.e. as the time-dependent expectation values of the center-of-mass coordinate and velocity, $\mathbf{R}(t)$ and $\mathbf{V}(t)$, such that $\mathbf{R}(t) - \mathbf{R}(t') = \int_{t'}^t \mathbf{V}(s) ds$. We are concerned with the steady transport under an irradiation of single frequency and focus on the photon-induced dc resistivity and the energy absorption of the HF field. These quantities are directly related to the time-averaged and/or base-frequency oscillating components of the center-of-mass velocity. Although higher harmonics of the current may affect the dc and lower harmonic terms of the drift velocity through entering the damping force and energy exchange rates in the resulting equations, in an ordinary semiconductor the power of even the third harmonic current is rather weak as compared to the fundamental. For the HF field intensity in the experiments, the effect of higher harmonic current is safely negligible. Hence, it suffices to assume that the center-of-mass velocity, i.e. the electron drift velocity, consists of a dc part \mathbf{v}_0 and a stationary time-dependent part $\mathbf{v}(t)$ of the form

$$\mathbf{V}(t) = \mathbf{v}_0 + \mathbf{v}_1 \cos(\omega t) + \mathbf{v}_2 \sin(\omega t). \quad (3)$$

With this, the exponential factor in the operator equations can be expanded in terms of Bessel functions $J_n(x)$:

$$e^{-i\mathbf{q} \cdot \int_{t'}^t \mathbf{V}(s) ds} = \sum_{n=-\infty}^{\infty} J_n^2(\xi) e^{i(\mathbf{q} \cdot \mathbf{v}_0 - n\omega)(t-t')} + \sum_{m \neq 0} e^{im(\omega t - \varphi)} \sum_{n=-\infty}^{\infty} J_n(\xi) J_{n-m}(\xi) e^{i(\mathbf{q} \cdot \mathbf{v}_0 - n\omega)(t-t')}.$$

Here $\xi \equiv \sqrt{(\mathbf{q}_{\parallel} \cdot \mathbf{v}_1)^2 + (\mathbf{q}_{\parallel} \cdot \mathbf{v}_2)^2} / \omega$ and $\tan \varphi = (\mathbf{q} \cdot \mathbf{v}_2) / (\mathbf{q} \cdot \mathbf{v}_1)$. On the other hand, for 2D systems having electron sheet density of order of 10^{15} m^{-2} , the intra-band and inter-band Coulomb interactions are sufficiently strong that it is adequate to describe the relative-electron transport state using a single electron temperature T_e . Except this, the electron-electron interaction is treated only in a mean-field level under random phase approximation (RPA).^{13,14} For the determination of unknown parameter \mathbf{v}_0 , \mathbf{v}_1 , \mathbf{v}_2 , and T_e , it suffices to know the damping force up to the base frequency oscillating term $\mathbf{F}(t) = \mathbf{F}_0 + \mathbf{F}_s \sin(\omega t) + \mathbf{F}_c \cos(\omega t)$, and the energy-related quantities up to the time-average term. We finally obtain the force and energy balance equations:

$$0 = N_e e \mathbf{E}_0 + N_e e (\mathbf{v}_0 \times \mathbf{B}) + \mathbf{F}_0, \quad (4)$$

$$\mathbf{v}_1 = \frac{e \mathbf{E}_s}{m\omega} + \frac{\mathbf{F}_s}{N_e m \omega} - \frac{e}{m\omega} (\mathbf{v}_2 \times \mathbf{B}), \quad (5)$$

$$-\mathbf{v}_2 = \frac{e \mathbf{E}_c}{m\omega} + \frac{\mathbf{F}_c}{N_e m \omega} - \frac{e}{m\omega} (\mathbf{v}_1 \times \mathbf{B}), \quad (6)$$

$$N_e e \mathbf{E}_0 \cdot \mathbf{v}_0 + S_p - W = 0. \quad (7)$$

Here

$$\mathbf{F}_0 = \sum_{\mathbf{q}_{\parallel}} |U(\mathbf{q}_{\parallel})|^2 \sum_{n=-\infty}^{\infty} \mathbf{q}_{\parallel} J_n^2(\xi) \Pi_2(\mathbf{q}_{\parallel}, \omega_0 - n\omega) + \sum_{\mathbf{q}} |M(\mathbf{q})|^2 \sum_{n=-\infty}^{\infty} \mathbf{q} J_n^2(\xi) \Lambda_2(\mathbf{q}, \omega_0 + \Omega_{\mathbf{q}} - n\omega), \quad (8)$$

is the time-averaged damping force, $S_p = \frac{1}{2} N_e e \mathbf{E}_s \cdot \mathbf{v}_2$ is the time-averaged rate of the electron energy-gain from the HF field, which can be written in a form obtained from that of \mathbf{F}_0 by replacing the \mathbf{q}_{\parallel} factor with $n\omega$, and W is the time-averaged rate of the electron energy-loss due to coupling with phonons, whose expression can be obtained from the second term on the right-hand side of equation (8) by replacing the \mathbf{q}_{\parallel} factor with $\Omega_{\mathbf{q}}$, the energy of a wavevector \mathbf{q} phonon. The oscillating frictional force amplitudes $\mathbf{F}_s \equiv \mathbf{F}_{11} + \mathbf{F}_{22}$ and $\mathbf{F}_c \equiv \mathbf{F}_{21} - \mathbf{F}_{12}$ are given by ($\mu = 1, 2$)

$$\mathbf{F}_{1\mu} = \sum_{\mathbf{q}_{\parallel}} \mathbf{q}_{\parallel} \eta_{\mu} |U(\mathbf{q}_{\parallel})|^2 \sum_{n=-\infty}^{\infty} [J_n^2(\xi)]' \Pi_1(\mathbf{q}_{\parallel}, \omega_0 - n\omega) + \sum_{\mathbf{q}} \mathbf{q} \eta_{\mu} |M(\mathbf{q})|^2 \sum_{n=-\infty}^{\infty} [J_n^2(\xi)]' \Lambda_1(\mathbf{q}, \omega_0 + \Omega_{\mathbf{q}} - n\omega),$$

$$\mathbf{F}_{2\mu} = \sum_{\mathbf{q}_{\parallel}} \mathbf{q}_{\parallel} \frac{\eta_{\mu}}{\xi} |U(\mathbf{q}_{\parallel})|^2 \sum_{n=-\infty}^{\infty} 2n J_n^2(\xi) \Pi_2(\mathbf{q}_{\parallel}, \omega_0 - n\omega) + \sum_{\mathbf{q}} \mathbf{q}_{\parallel} \frac{\eta_{\mu}}{\xi} |M(\mathbf{q})|^2 \sum_{n=-\infty}^{\infty} 2n J_n^2(\xi) \Lambda_2(\mathbf{q}, \omega_0 + \Omega_{\mathbf{q}} - n\omega).$$

In these expressions, $\eta_{\mu} \equiv \mathbf{q}_{\parallel} \cdot \mathbf{v}_{\mu} / \omega \xi$; $\omega_0 \equiv \mathbf{q}_{\parallel} \cdot \mathbf{v}_0$; $U(\mathbf{q}_{\parallel})$ and $M(\mathbf{q})$ stand for effective impurity and phonon scattering potentials, $\Pi_2(\mathbf{q}_{\parallel}, \Omega)$ and $\Lambda_2(\mathbf{q}, \Omega) = 2\Pi_2(\mathbf{q}_{\parallel}, \Omega)[n(\Omega_{\mathbf{q}}/T) - n(\Omega/T_e)]$ are the imaginary parts of the spectra of the electron density correlation function and the electron-phonon correlation function in the presence of the magnetic field, $n(x) \equiv 1/[\exp(x) - 1]$ is the Bose function. $\Pi_1(\mathbf{q}_{\parallel}, \Omega)$ and $\Lambda_1(\mathbf{q}, \Omega)$ are the real parts of the spectra of these two correlation functions. The effect of interparticle Coulomb interactions are taken into account to the degree of energy level broadening and RPA screening.

The HF field enters through the argument ξ of the bessel functions in expressions of \mathbf{F}_0 , $\mathbf{F}_{\mu\nu}$, W and S_p . Compared with those without the HF field ($n = 0$ term only),¹⁵ we see that in an electron gas having impurity and/or phonon scattering (otherwise homogeneous), a HF field of frequency ω opens additional channels for electron transition: an electron in a state can absorb or emit one or several photons and scattered to a different state with the help of impurities and/or phonons. The sum over $|n| \geq 1$ represents contributions of single and multiple photon processes of frequency- ω photons. These photon-assisted scatterings help to transfer energy from the HF field to the electron system (S_p) and give rise to additional damping force on the moving electrons. Note that \mathbf{v}_1 and \mathbf{v}_2 always exhibit CR in the range $\omega \sim \omega_c$, as can be seen from Eqs.(5) and (6) rewritten in the form

$$\begin{aligned} \mathbf{v}_1 &= (1 - \omega_c^2/\omega^2)^{-1} \left\{ \frac{e}{m\omega} \left[\mathbf{E}_s + \frac{e}{m\omega} (\mathbf{E}_c \times \mathbf{B}) \right] + \frac{1}{N_e m\omega} \left[\mathbf{F}_s + \frac{e}{m\omega} (\mathbf{F}_c \times \mathbf{B}) \right] \right\}, \\ \mathbf{v}_2 &= (\omega_c^2/\omega^2 - 1)^{-1} \left\{ \frac{e}{m\omega} \left[\mathbf{E}_c - \frac{e}{m\omega} (\mathbf{E}_s \times \mathbf{B}) \right] + \frac{1}{N_e m\omega} \left[\mathbf{F}_c - \frac{e}{m\omega} (\mathbf{F}_s \times \mathbf{B}) \right] \right\}. \end{aligned}$$

Therefore, ξ may be significantly different from $e\mathbf{q}_{\parallel} \cdot \mathbf{E}_s / (m\omega^2)$, the argument of the bessel functions in the case without a magnetic field¹⁵ or with a magnetic field in Voigt configuration, where the electron motion is not affected by the magnetic field.

Eqs.(4)-(7) can be used to describe the transport and optical properties of magnetically-biased quasi-2D semiconductors subjected to a dc field and a HF field. The response of the linear dc resistivity to a HF radiation is obtained in the the weak dc field limit. Taking \mathbf{v}_0 to be in the x direction, $\mathbf{v}_0 = (v_{0x}, 0, 0)$, and expanding the equation (4) to the first order in v_{0x} , we get the transverse and longitudinal resistivities $R_{xy} \equiv E_{0y}/N_e e v_{0x}$

and $R_{xx} \equiv E_{0x}/N_e e v_{0x}$ as

$$R_{xy} = B/N_e e, \quad (9)$$

$$\begin{aligned} R_{xx} &= - \sum_{\mathbf{q}_{\parallel}} q_x^2 \frac{|U(\mathbf{q}_{\parallel})|^2}{N_e^2 e^2} \sum_{n=-\infty}^{\infty} J_n^2(\xi) \frac{\partial \Pi_2}{\partial \Omega} \Big|_{\Omega=n\omega} \\ &\quad - \sum_{\mathbf{q}} q_x^2 \frac{|M(\mathbf{q})|^2}{N_e^2 e^2} \sum_{n=-\infty}^{\infty} J_n^2(\xi) \frac{\partial \Lambda_2}{\partial \Omega} \Big|_{\Omega=\Omega_{\mathbf{q}}+n\omega} \quad (10) \end{aligned}$$

The parameters \mathbf{v}_1 , \mathbf{v}_2 and T_e in these expressions should be determined by solving equations (5), (6) and (7) with vanishing \mathbf{v}_0 . We see that although the transverse resistivity R_{xy} remains the classical form, the longitudinal resistivity R_{xx} would be strongly affected by the irradiation.

We calculate the $\Pi_2(\mathbf{q}_{\parallel}, \Omega)$ function of a 2D system in a magnetic field by means of Landau representation as¹⁶

$$\Pi_2(\mathbf{q}_{\parallel}, \Omega) = \frac{1}{2\pi l_B^2} \sum_{n,n'} C_{n,n'} (l_B^2 q_{\parallel}^2/2) \Pi_2(n, n', \Omega), \quad (11)$$

$$\begin{aligned} \Pi_2(n, n', \Omega) &= -\frac{2}{\pi} \int d\varepsilon [f(\varepsilon) - f(\varepsilon + \Omega)] \\ &\quad \times \text{Im}G_n(\varepsilon + \Omega) \text{Im}G_{n'}(\varepsilon), \quad (12) \end{aligned}$$

where $l_B = \sqrt{1/|eB|}$ is the magnetic length, $C_{n,n+l}(Y) \equiv n![(n+l)!]^{-1} Y^l e^{-Y} [L_n^l(Y)]^2$ with $L_n^l(Y)$ the associate Laguerre polynomial, $f(\varepsilon) = \{\exp[(\varepsilon - \mu)/T_e] + 1\}^{-1}$ the Fermi distribution function, and $\text{Im}G_n(\varepsilon)$ is the imaginary part of the Green's function, or the DOS, of the Landau level n . The real part functions $\Pi_1(\mathbf{q}_{\parallel}, \Omega)$ and $\Lambda_1(\mathbf{q}_{\parallel}, \Omega)$ can be obtained from their imaginary parts via the Kramers-Kronig relation.

In principle, to obtain the Green's function $\text{Im}G_n(\varepsilon)$, a self-consistent calculation has to be carried out from the Dyson equation for the self-energy with all the scattering mechanisms included. The resultant G_n is generally a complicated function of the magnetic field, temperature, and Landau-level index n , also dependent on the relative strength of the impurity and phonon scatterings.¹⁸ In the present study we do not attempt a self-consistent calculation of $G_n(\varepsilon)$. Instead, we choose a Gaussian-type form¹¹ for the purpose of demonstrating the observed oscillations (ε_n is the energy of the n -th Landau level)

$$\text{Im}G_n(\varepsilon) = -(\pi/2)^{\frac{1}{2}} \Gamma^{-1} \exp[-(\varepsilon - \varepsilon_n)^2/(2\Gamma^2)] \quad (13)$$

with a broadening parameter $\Gamma = (2e\omega_c \alpha / \pi m \mu_0)^{1/2}$, where μ_0 is the linear mobility in the absence of the magnetic field and $\alpha > 1$ is a semiempirical parameter to take account the difference of the transport scattering time determining the mobility μ_0 , from the single particle lifetime which is related to all kinds of interparticle collisions.^{2,4,6}

The microwave field intensity required for resistivity oscillation in these high-mobility samples is moderate. For simplicity we neglect the heating of electrons, thus exclude the conventional CR in photoresistivity. The

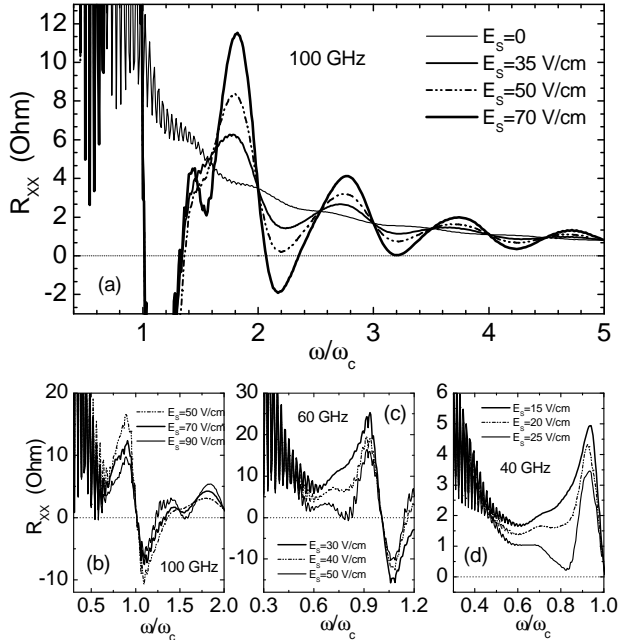


FIG. 1: The longitudinal magnetoresistivity R_{xx} of a GaAs-based 2DEG subjected to a HF field $E_s \sin(\omega t)$. The parameters are: temperature $T = 1$ K, electron density $N_e = 3.0 \times 10^{11} \text{ cm}^{-2}$, dc mobility $\mu_0 = 2.5 \times 10^7 \text{ cm}^2 \text{ V}^{-1} \text{ s}^{-1}$, and the broadening coefficient $\alpha = 12.5$.

magnetoresistivity R_{xx} can then be obtained directly from Eq. (11) with $T_e = T$. Calculations were carried out with multiphoton contributions included.

Fig. 1 shows the calculated longitudinal resistivity R_{xx} versus $\omega/\omega_c \equiv \gamma_f$ subjected to a MW radiation of frequency $\omega/2\pi = 100$ GHz at four values of amplitudes: $E_s = 0, 35, 50$ and 70 V/cm. SdH oscillations show up strongly at high ω_c side, especially in the dark case ($E_s = 0$), and then gradually decay away as ω_c increases. All three resistivity curves with HF illumination exhibit pronounced smooth oscillation. The oscillation period is accurately $\gamma_f = 1$, with the maxima around $\gamma_f = j - 0.2$ and minima around $\gamma_f = j + 0.2$ ($j = 2, 3, 4, 5$), except

the first ($j = 1$) maximum and minimum which locate closer to $\gamma_f = 1$. The magnitude of the oscillation increases with increasing HF field intensity at low power as can be seen for $\gamma_f > 1.5$, and may saturates even reverses at higher power, as is the case in the vicinity of $\gamma_f = 1$, where the CR greatly enhances the effective amplitude of the HF field in photon-assisted scatterings, such that $E_s = 35$ V/cm curve exhibits the largest amplitude. Resistivity gets into negative value for $E_s = 70$ V/cm around the minima at $j = 1, 2$ and 3 , for $E_s = 50$ V/cm at $j = 1$ and 2 , and for $E_s = 35$ V/cm at $j = 1$. Note that four curves are crossing at points $\gamma_f = 1, 2, 3, 4, 5$ and at nearly half- ω_c points for $\gamma_f > 2.5$. All these features are in fairly good agreement with experimental findings.^{2,3} Furthermore, there appears a shoulder around $\gamma_f = 1.4$ on the curves of $E_s = 35$ and 50 V/cm, and it develops into a secondary peak in the $E_s = 70$ V/cm curve. This seems already observed in the experiment (Fig. 2 in Ref. 3). The valley between $\gamma_f = 1.4$ and 1.8 peaks can descend down to negative as E_s increasing further (Fig. 1b). The appearance of the secondary peak is relevant with multiphoton assisted process.

Radiation-induced resistivity structures at $\gamma_f < 1$ show up more clearly in the $\omega/2\pi = 60$ GHz case. As seen in Fig. 1c, a minimum around $\gamma_f = 0.6$ exists at all three curves. With increasing MW strength there appear a peak around $\gamma = 0.7$ and a valley around $\gamma_f = 0.8$, which can develop into negative value. In the case of $\omega/2\pi = 40$ GHz, similar peaks and valleys also show up (Fig. 1d).

Calculation has also been carried using a Lorentz-type DOS function. We find that, although the oscillating amplitude and the exact peak and valley positions (δ_1 and δ_2) somewhat depend on the form of the DOS function, the basic features of the radiation-induced magnetoresistivity oscillation remain the same.

This work was supported by the National Science Foundation of China, the Special Funds for Major State Basic Research Project, and the Shanghai Municipal Commission of Science and Technology.

- ¹ M.A. Zudov, R.R. Du, J.A. Simmons, and J.L. Reno, Phys. Rev. B **64**, 201311(R) (2001).
- ² R.G. Mani, J.H. Smet, K. von Klitzing, V. Narayanamurti, W.B. Johnson, and V. Umansky, Nature **420**, 646 (2002).
- ³ M.A. Zudov, R.R. Du, L.N. Pfeiffer, and K.W. West, Phys. Rev. **90**, 046807 (2003).
- ⁴ A.C. Durst, S. Sachdev, N. Read, and S.M. Girvin, preprint, cond-mat/0301569.
- ⁵ A.V. Andreev, I.L. Aleiner, and A.J. Millis, preprint, cond-mat/0302063.
- ⁶ P.W. Anderson and W.F. Brinkman, preprint, cond-mat/0302129.
- ⁷ J. Shi and X.C. Xie, preprint, cond-mat/0302393.
- ⁸ J.C. Phillips, preprint, cond-mat/03
- ⁹ A.A. Koulakov, and M.E. Raikh, preprint,

- cond-mat/0302465.
- ¹⁰ W. Kohn, Phys. Rev. **123**, 1242 (1961).
- ¹¹ T. Ando, Phys. Rev. Lett. **36**, 1383 (1976).
- ¹² P.K. Tien and J.P. Gordon, Phys. Rev. **129**, 647 (1963).
- ¹³ X. L. Lei and C. S. Ting, Phys. Rev. B **32**, 1112 (1985).
- ¹⁴ X. L. Lei, J. L. Birman, and C. S. Ting, J. Appl. Phys. **58**, 2270 (1985).
- ¹⁵ X. L. Lei, J. Appl. Phys. **84**, 1396 (1998); J. Phys.: Condens. Matter **10**, 3201 (1998).
- ¹⁶ C. S. Ting, S. C. Ying, and J. J. Quinn, Phys. Rev. B **14**, 5394 (1977).
- ¹⁷ T. Ando, A.B. Fowler, and F. Stern, Rev. Mod. Phys. **54**, 437 (1982).
- ¹⁸ D.R. Leadley et al. Phys. Rev. B **48**, 5457 (1993).